Impact of the hydrophobicity of the particles on the formation and behavior of oil particle aggregates (OPA)

Wen Ji[1], Lin Zhao[2], Kenneth Lee[3], Thomas King[3], Brian Robinson[3], and Michel C. Boufadel[1*]

1: Center for Natural Resources, Department of Civil and Environmental Engineering, New Jersey Institute of Technology, 323 MLK Blvd, Newark, NJ 07102.
boufadel@gmail.com; http://nrdp.njit.edu
2: ExxonMobil Upstream Research Company, Science 1-6B.324, 22777 Springwoods Village Parkway, Houston, TX 77389.
3: Bedford Institute of Oceanography, Department of Fisheries and Oceans, 1 Challenger Dr, Dartmouth, NS B2Y 4A2, Canada 1006.

ABSTRACT 689143

Oil droplets in marine environment interact with particles to form oil particle aggregates (OPA). As it was argued that the hydrophobicity of particles impacts the formation of OPA and subsequently the entrapment of oil and the transport of OPA, this study altered the hydrophobicity of kaolinite through the addition of chitosan and the contact angle was increased from 28.8° to 57.3°. Modified kaolinite was mixed with 500 mg/L crude oil in 200 rpm for 3 hours, then bottom layer was separated and extracted. Observations of the settled OPA microscale structure and calculations of oil trapping efficiency (OTE) were accomplished. Results indicated that with higher hydrophobicity of kaolinite, oil droplets were maintained in larger sizes in OPAs. This could increase the buoyancy of formed OPAs, thus decrease the amount of settled OPAs.

1. INTRODUCTION

After oil spills in aquatic environment, some oil droplets would be dispersed in the water column due to mixing energy or turbulence (Hinze 1955, Fitzpatrick et al. 2015, Li et al. 2016, Zhao et al. 2017c). Once spilled into a water body with turbulence created by waves or currents, floating oil of moderate to light viscosity can break up into droplets and reach a stable droplet size distribution (DSD) relatively quickly, normally in less than tens of minutes (Zhao et al. 2014). Suspended particles in the water column can interact with these droplets to form microscopic oil particles aggregates (OPAs) (Lee et al. 2003). OPA formation process has been observed in various aquatic environments like freshwater systems (EPA 2013, Dollhopf1 et al. 2014, Fitzpatrick et al. 2015), shorelines (Lee et al. 2003, Boufadel et al. 2019a), or deeper waters of oceans (White et al. 2012, Daly et al. 2016). In all of these systems, mixing energy due to breaking waves and other turbulent forces, such as shear generation from the streambed (Boufadel et al. 2019b) would also facilitate the interaction between these sediments and floating oil (Gustitus et al. 2017).

The efficiency of OPA formation is affected by the physical and chemical properties of particles such as available interlayer spaces and surface properties (Jaynes et al. 1991, Stoffyn-Egli et al. 2002, Loh et al. 2014). Clay is termed as the finest fraction of sediment composed of particles with diameters less than 2 μm irrespective of their chemical compositions (Friedman et al. 1992, Stoffyn-Egli et al. 2002). Particles such as kaolinite, montmorillonite, quartz, silica, are common in OPA formation but kaolinite and quartz are more frequently used in laboratory work (Khelifa et al. 2002, Muschenheim et al. 2002, Omotoso et al. 2002, Stoffyn-Egli et al. 2002), whereas kaolinite has strong cation exchange capacity and therefore easier to form a hydrophobic surface (Stoffyn-Egli et al. 2002) to develop OPAs. The contact angle of the water-air interface on the sediment particle is an important indication of the hydrophobicity of the particle, and the free

energy of adsorption of particles is given by the following expression (Leal-Calderon et al. 2008, Owoseni et al. 2015, Zhao et al. 2016):

$$\Delta G_d = \pi r^2 \gamma_{ow} \left(1 - \left|\cos\left(\theta_{wo}\right)\right|\right)^2 \quad (1)$$

where r is the radius of the particles, γ_{ow} is the oil-water interfacial tension, and θ_{wo} is the equilibrium contact angle measured through the water phase, and larger values imply larger hydrophobicity. As shown in Eq. 1, the formation of OPA is strongly related to the contact angle (θ_{wo}) at the water-oil-particle interfaces (Owoseni et al. 2015, Gaweł et al. 2016). For this reason, the goal of the current research is to assess the impact of the hydrophobicity of kaolinite particles on the formation of OPA.

2. METHODS

In all these experiments, the oil was ANS (Alaska North Slope) crude oil that was weathered (10%) in the air (in a fume hood). The oil concentration (C_o) was kept 500 mg/L in filtered artificial seawater as the continuous medium. The artificial seawater was synthetic by using ultrapure deionized water with a precalculated weight of ocean sea salt (Lake Products Co., Mo, U.S.) to obtain a salinity of ~33 ppt (parts per thousand) and filtered through 0.45 μm pore size filter to get rid of undissolved contaminants. The oil and water were mixed in 200 mL baffled flasks and shaking by an orbital shaker (Thermo Scientific, MaxQ 2000) at the rotation speed 200 rpm for 3 hours. The energy dissipation rate at this rotation speed was obtained from the work of Zhao et al. (2015) of 0.67 Watt/Kg. The experimental matrix is reported in Table 1.

Table 1. Experiment setup in OPA formation tests

Particle	Diameter (μm)	Contact Angle (°)	Particle Conc. (mg/L)	Oil Conc. (mg/L)
kaolinite	~7	28.8	500	500
		30.6	500	500
		37.7	500	500
		57.3	500	500

The kaolinite (Sigma-Aldrich) we purchased was in the shape of either plate or rod (Figure 1) with a median equivalent diameter dp50 of $\sim 7\ \mu m$ (the diameter equivalent to spherical particles based on the volume; and dp50 was the 50% point of equivalent diameter in the cumulative volume fraction). The kaolinite particle is moderately hydrophilic with a contact angle of ~28.8° and the density is reported at ~2630 kg/m^3 (Zhao et al. 2017a).

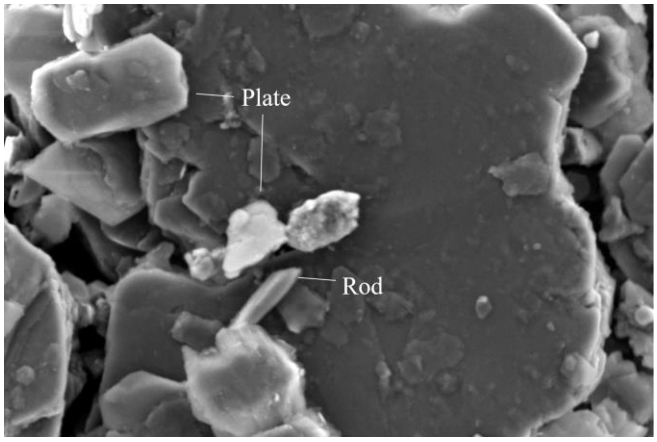

Fig. 1. Scanning Electron Microscopy at ×8000 magnification of kaolinite particles, which are in the shape of plate or rod.

The hydrophobicity of kaolinite was altered using chitosan, glacial acetic acid ($\geq 99.7\%$) and sodium hydroxide (Sigma-Aldrich, U.S.). Chitosan was purchased from Sigma-Aldrich and had a molecular weight 190~310 kDa. Dichloromethane ($\geq 99.9\%$) was purchased from Fisher Scientific as the solvent to extract oil from artificial seawater. All these chemicals were used as received. The organic carbon content in kaolinite was zero, confirmed by the lack of fluorescent emission in the confocal microscope. Four parallel experiments were conducted to evaluate

hydrophobicity impacts. The kaolinite particles were modified at chitosan to kaolinite the mass ratio m_c/m_p of 0; 0.01; 0.02; 0.04. Namely, the modification method was similar to that by Owoseni et al. (2015) that chitosan and kaolinite was firstly mixed in an acid solution by adding glacial acetic acid to adjust the pH to ~3.7. After mixing for 24 hours, the pH level of the solution was adjusted to neutral using sodium hydroxide aqueous solution (0.1 mol/L). Then modified kaolinite was allowed to settle, shown as Figure 2. After centrifuge and filtration, the modified kaolinite was washed by pure ethanol three times and dried in fume hood overnight. The kaolinite was then ground and mixed with deionized water, and 1 mL aqueous mixture was taken and dropped carefully on a glass plate and left for dry. A thin layer of these modified particles was produced after dried, and then one drop of deionized water was slowly placed on them and images of these process were taken to analyse the contact angles by the software ImageJ, as shown in Figure 3. And the entire process was shown as the flowchart in Fig. 4. Their contact angles were found to be 28.8°; 30.6°; 37.7°; 57.3° at the chitosan/kaolinite mass ratio 0, 0.01, 0.02 and 0.04 respectively.

Figure 2. Kaolinite modified by chitosan at different mass ratios were left settling after 12 hours.

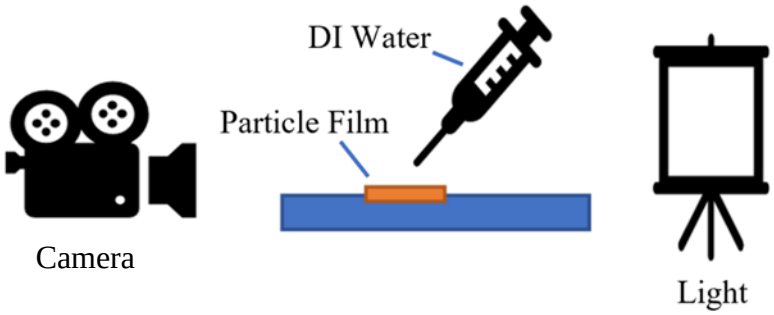

Figure 3. Schematic of (rement setup.

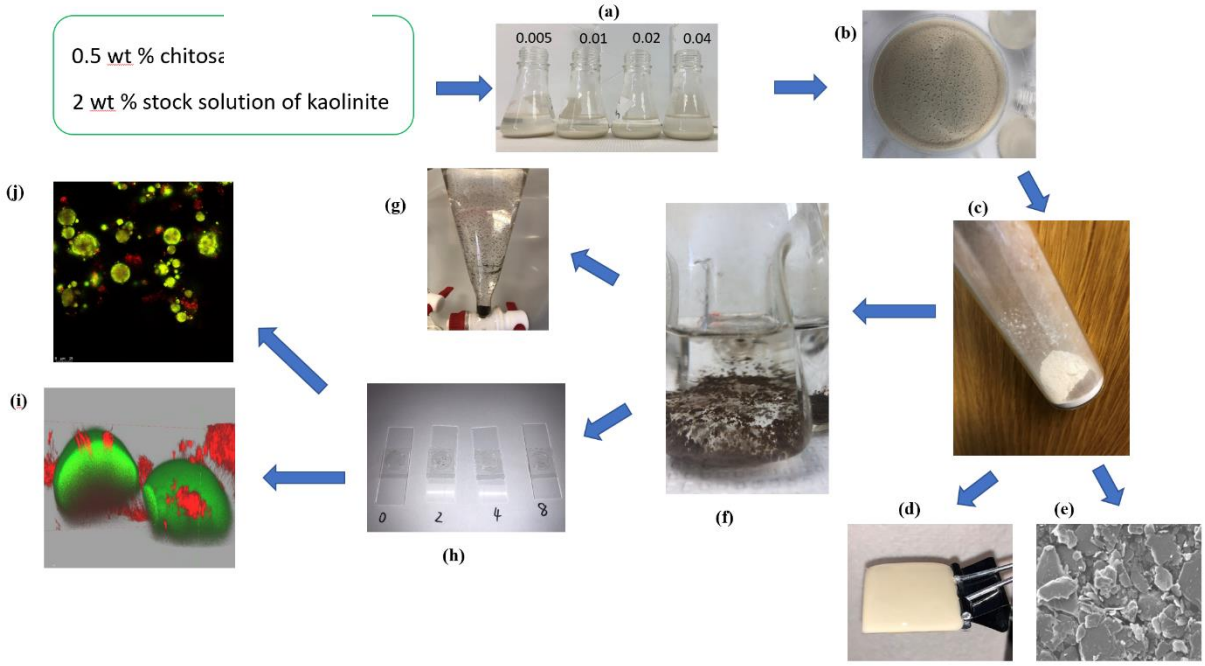

Figure 4. Flow chart of kaolinite employed OPA formation experiment with each step of: a) prepare kaolinite particles to have different hydrophobicity by mixing chitosan and initial kaolinite solution; b) produced kaolinite in the baffled flask; c) centrifuge, filter, dried and ground kaolinite; d) create a kaolinite film by aqueous solution to measure contact angle as shown in Fig. 3; e) SEM scanning to understand the shape of kaolinite as Fig. 1; f) apply different particles in OPA formation experiments in baffled flasks; g) after mixing, transfer the mixture into separatory funnels to measure the oil amount in different layers; h) take OPA samples from the bottom and make confocal microscope slides; j) 2D scanning of confocal microscope where fluorescent parts are oil droplets and red parts are particles; i) 3D scanning of OPAs by clipping function to obtain the cross-section view.

The seeding oil concentration and particle concentration were both 500 mg/L, and were achieved as follows: a volume of 100 mL filtered artificial seawater was added into baffled flasks,

and 0.05 g (± 0.0005 g) ground kaolinite was measured and mixed with artificial seawater. The oil was seeded by a positive displacement pipette at the volume of 58.5 μL (50 mg with the density 0.85 g/mL). Following the seeding the flasks were placed on an orbital shaker for 3 hours each and the shaking speed was 200 rpm.

The oil trapping efficiency (OTE) was obtained to justify the oil amount trapped by particles in different layers, namely the negatively buoyant OPAs, the suspended OPAs and the OPAs floating on the water surface. The test includes separation, extraction and UV-Vis spectrophotometer detection of hydrocarbons. After the mixing, the mixture in the OPA formation apparatus was decanted to a separatory funnel and washed gently by 50 mL artificial seawater to obtain all the materials in initial flasks. After the settlement overnight, the formed OPAs were mostly settled on the bottom as the negatively buoyant OPAs. Some oil or buoyant OPAs stayed on the surface and small amount of OPAs kept suspended in water. The bottom layer was taken separately (shown in Figure 5a) and extracted by dichloromethane (DCM) three times. The extraction for different layers were scanned by UV-Vis spectrophotometer at three wavelengths 340 nm, 370 nm and 400 nm (Pan et al. 2017) to obtain the concentration of oil and hence calculated the amount of trapped oil in OPAs. Duplicates were tested and averaged to control the error.

To understand the interaction mechanisms of OPAs, confocal microscopy was applied to detect the micro scale structure of them. Negatively buoyant OPAs were taken from the bottom of the flasks and transferred to microscope slides. The slides were then covered by a coverslip with sealed chamber gasket at 20 mm diameter and a 150 μm deep well. The coverslip can protect the morphology of the specimen (Zhao et al. 2017b), as shown as Figure 5b. A confocal microscope (Leica TCS SP8) was used to obtain the three-dimensional (3D) structure of OPA specimen, as

this microscope is able to scan a thin cross-section of the specimen (several nano-meters in depth) by excluding most of the light from the specimen that is not from the microscope's focal plane (Zhao et al. 2017b). In this study, simultaneous excitation wavelengths of 488 and 638 nm were used. The signal emitted in the range of 483-603 nm was recorded in the green channel to represent the fluorescent oil, whereas the signal in the wavelengths of 609-672 nm in the red channel represent the particles. Scans were obtained through a 40× oil immersion objective lens in the focal planes 0.1~0.35 μm apart to reveal the 3D structures of the OPA. All the OPA images were obtained and analysed using the commercial software LAS X provided by Leica Microsystems. The former OTE measurement is macroscopic while this 3D measurement is microscopic, and thus the investigation allows us to both explore the fundamental properties of OPA formation along with the practical implications.

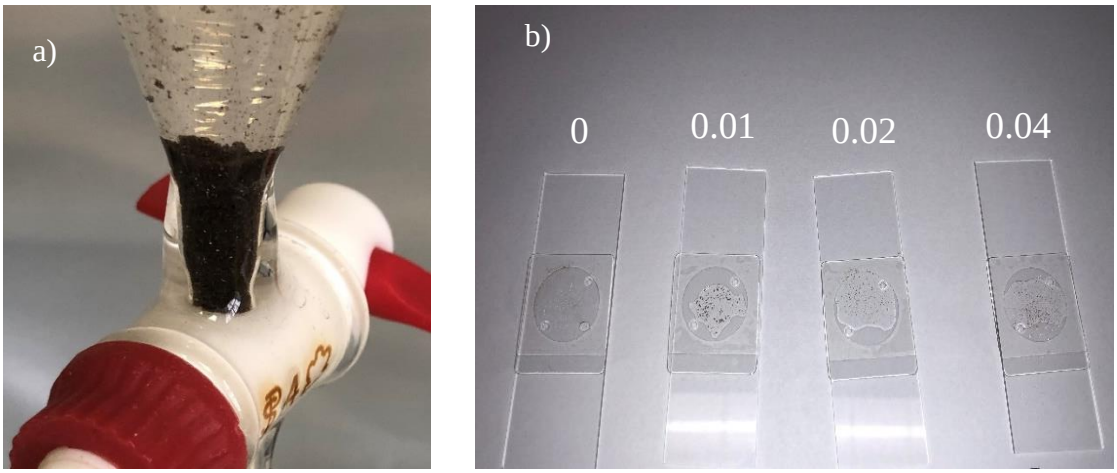

Fig 5. Sampling process for: a) OTE test after phase separation (the particle employed in this case has the contact angle of 37.7 degree); b) confocal microscopy test (samples had the contact angle 28.8°; 30.6°; 37.7°; 57.3° from left to right respectively).

3. RESULTS

This experiment aimed to compare formed OPAs by modified kaolinite in different levels of hydrophobicity. Figure 6 shows the OTE percentage for the bottom layers by kaolinite of various

hydrophobicity (refer to the contact angles) in OPA formation. The results show that the mass of settled OPA decreased from 94.00% to 59.44% when the angle increased from 28.8 until reaching 37.7 degrees. It then increased slightly to 65.90% when the angle was 57.3 degree. An explanation would be that when the particles become too hydrophobic (57.3°), the particles bunch together and thus interact less with the oil. This was indeed observed in Zhang et al. (2010).

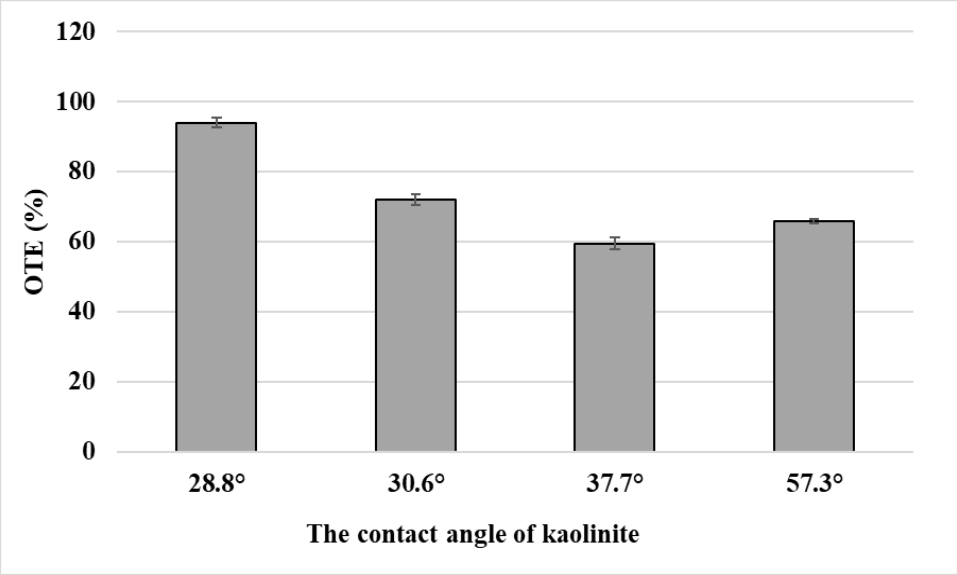

Fig 6. Impact of the hydrophobicity, expressed through the contact angle, on the OTE of bottom layer in the baffled flasks after 3 hours mixing at 200 rpm. The concentration of oil and particles were both 500 mg/L. The error bars were obtained based on the standard deviation of three replicate experiments, and the highest error bar value was 1.75%.

Figure 7 shows the 3D structure of particles penetrating oil droplets in four cases. The penetration of particles into the oil droplets occurred in all these cases. When less hydrophobic particles were mixed with oil, the particles were not always interacting with oil droplets. Instead, these particles integrated with each other and were seen as “free particles”. When scanning the specimen by confocal microscope, these free particles widely existed when kaolinite with lower contact angles were employed. When the hydrophobicity increased, there were less free particles and the average sizes of free ones decreased (less amount of separated kaolinite particles integrated).

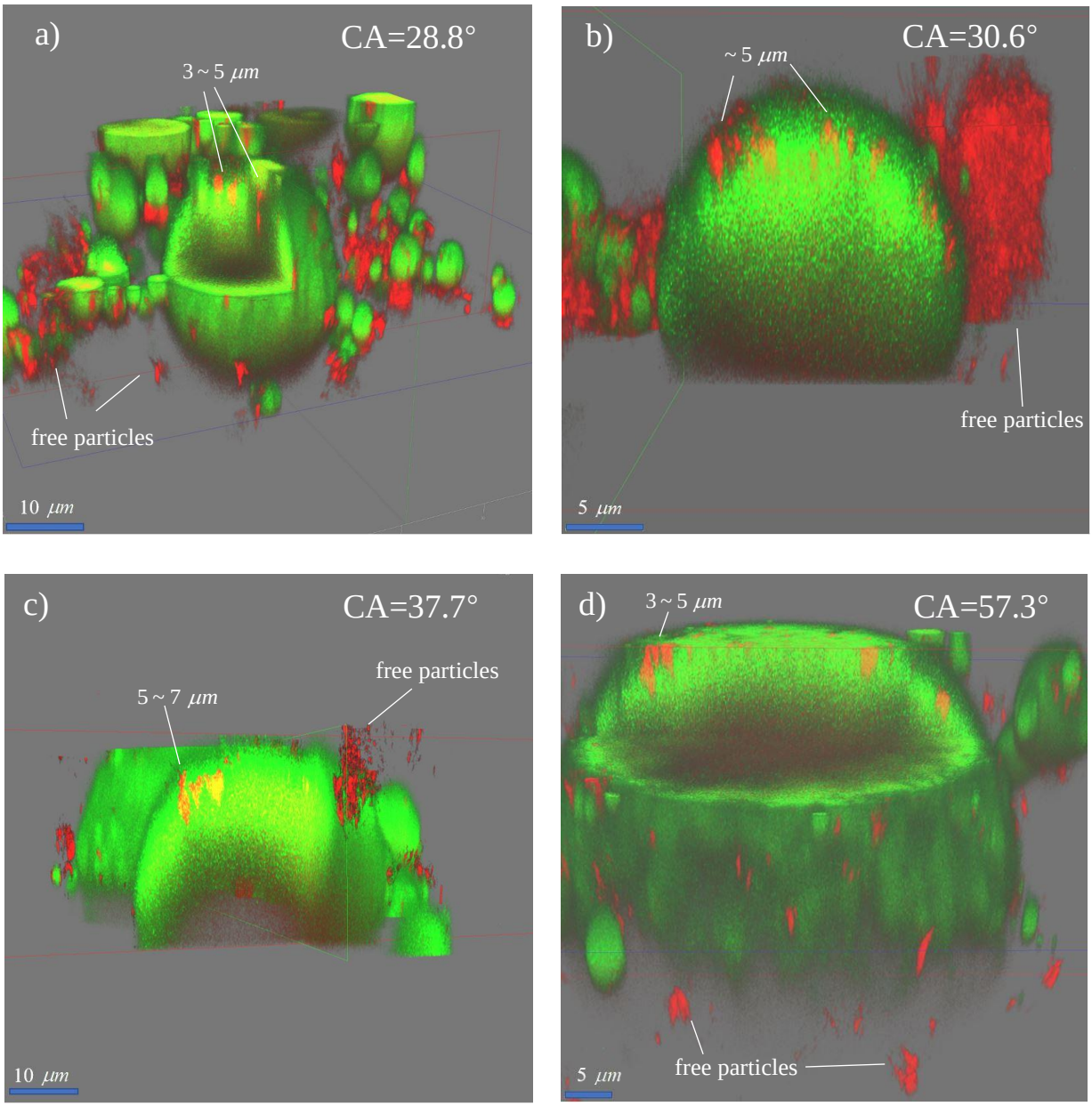

Fig. 7. Confocal microscopy results of OPA formed by kaolinite of different hydrophobicity, expressed as contact angle (CA, the larger the more hydrophobic) at: a) 28.8; b) 30.6; c) 37.7; d) 57.3 degree. The green color stands for oil droplets while red color means particles.

4. DISCUSSION

By changing the hydrophobicity of kaolinite, the interaction between oil droplets and particles could be learned. Particles come in different hydrophobicity due to the environmental conditions. With higher hydrophobicity of kaolinite, oil droplets were maintained in larger sizes

in OPAs. This could increase the buoyancy of formed OPAs, thus decrease the amount of settled OPAs, as shown in Figs 6.

When oil spills near shore environment, where the particle density is higher and mixing energy gets higher, the OPA interaction would happen more frequently as both the collision frequency and mixing intensity gets higher. When the OPA forms in such an environment, most of the OPAs would be negatively buoyant and settle down to the sea bed. The penetration happens when kaolinite was employed in the interaction with oil droplets, especially those with higher hydrophobicity. And with higher hydrophobicity, the penetration depth increases to as large as 7 μm. But when the most hydrophobic kaolinite employed, the penetration depth decreased to 3~5 μm. As penetration happened a lot even in one single oil droplet, there should be further data collection and modelling to help develop a relationship between the depth and the particle and mixing properties.

REFERENCE

Boufadel, M., X. Geng, C. An, E. Owens, Z. Chen, K. Lee, E. Taylor and R. C. Prince (2019a). "A Review on the factors affecting the deposition, retention, and biodegradation of oil stranded on beaches and guidelines for designing laboratory experiments " Current Pollution Reports **in press**.

Boufadel, M. C., F. Fitzpatrick, F. Cui and K. Lee (2019b). "Computation of the Mixing Energy in Rivers for Oil Dispersion." Journal of Environmental Engineering **145**(10): 06019005.

Daly, K. L., U. Passow, J. Chanton and D. Hollander (2016). "Assessing the impacts of oil-associated marine snow formation and sedimentation during and after the Deepwater Horizon oil spill." Anthropocene **13**: 18-33.

Dollhopf1, R. H., F. A. Fitzpatrick, J. W. Kimble1, D. M. Capone, T. P. Graan, R. B. Zelt and R. Johnson (2014). Response to heavy, non-floating oil spilled in a Great Lakes river environment: a multiple-lines-of-evidence approach for submerged oil assessment and recovery. International Oil Spill Conference Proceedings, American Petroleum Institute.

EPA (2013). "Dredging Begins On Kalamazoo River: Enbridge Oil Spill Marshall, Michigan."

Fitzpatrick, F. A., M. C. Boufadel, R. Johnson, K. W. Lee, T. P. Graan, A. C. Bejarano, Z. Zhu, D. Waterman, D. M. Capone and E. Hayter (2015). Oil-particle interactions and submergence from crude oil spills in marine and freshwater environments: Review of the science and future research needs, US Geological Survey.

Friedman, G. M., J. E. Sanders and D. C. Kopaska-Merkel (1992). Principles of sedimentary deposits: stratigraphy and sedimentology, Macmillan College.

Gaweł, B., M. Nourani, T. Tichelkamp and G. Øye (2016). "Influence of the wettability of particles on the morphology and stability of crude oil–particle aggregates in synthetic produced water." Journal of Petroleum Science and Engineering **139**: 198-204.

Gustitus, S. A. and T. P. Clement (2017). "Formation, Fate, and Impacts of Microscopic and Macroscopic Oil-Sediment Residues in Nearshore Marine Environments: A Critical Review." Reviews of Geophysics **55**(4): 1130-1157.

Hinze, J. (1955). "Fundamentals of the hydrodynamic mechanism of splitting in dispersion processes." AIChE Journal **1**(3): 289-295.

Jaynes, W. and S. Boyd (1991). "Hydrophobicity of siloxane surfaces in smectites as revealed by aromatic hydrocarbon adsorption from water." Clays and Clay Minerals **39**(4): 428-436.

Khelifa, A., P. Stoffyn-Egli, P. S. Hill and K. Lee (2002). "Characteristics of oil droplets stabilized by mineral particles: effects of oil type and temperature." Spill Science & Technology Bulletin **8**(1): 19-30.

Leal-Calderon, F. and V. Schmitt (2008). "Solid-stabilized emulsions." Current Opinion in Colloid & Interface Science **13**(4): 217-227.

Lee, K., P. Stoffyn-Egli, G. H. Tremblay, E. H. Owens, G. A. Sergy, C. C. Guénette and R. C. Prince (2003). "Oil–mineral aggregate formation on oiled beaches: natural attenuation and sediment relocation." Spill Science & Technology Bulletin **8**(3): 285-296.

Li, X., H. Xu, J. Liu, J. Zhang, J. Li and Z. Gui (2016). "Cyclonic state micro-bubble flotation column in oil-in-water emulsion separation." Separation and Purification Technology **165**: 101-106.

Loh, A., W. J. Shim, S. Y. Ha and U. H. Yim (2014). "Oil-suspended particulate matter aggregates: Formation mechanism and fate in the marine environment." Ocean Science Journal **49**(4): 329-341.

Muschenheim, D. and K. Lee (2002). "Removal of oil from the sea surface through particulate interactions: review and prospectus." Spill Science & Technology Bulletin **8**(1): 9-18.

Omotoso, O. E., V. A. Munoz and R. J. Mikula (2002). "Mechanisms of crude oil–mineral interactions." Spill Science & Technology Bulletin **8**(1): 45-54.

Owoseni, O., Y. Zhang, Y. Su, J. He, G. L. McPherson, A. Bose and V. T. John (2015). "Tuning the Wettability of Halloysite Clay Nanotubes by Surface Carbonization for Optimal Emulsion Stabilization." Langmuir **31**(51): 13700-13707.

Pan, Z., L. Zhao, M. C. Boufadel, T. King, B. Robinson, R. Conmy and K. Lee (2017). "Impact of mixing time and energy on the dispersion effectiveness and droplets size of oil." Chemosphere **166**: 246-254.

Stoffyn-Egli, P. and K. Lee (2002). "Formation and Characterization of Oil–Mineral Aggregates." Spill Science & Technology Bulletin **8**(1): 31-44.

White, H. K., P.-Y. Hsing, W. Cho, T. M. Shank, E. E. Cordes, A. M. Quattrini, R. K. Nelson, R. Camilli, A. W. Demopoulos and C. R. German (2012). "Impact of the Deepwater Horizon oil spill on a deep-water coral community in the Gulf of Mexico." Proceedings of the National Academy of Sciences **109**(50): 20303-20308.

Zhang, H., M. Khatibi, Y. Zheng, K. Lee, Z. Li and J. V. Mullin (2010). "Investigation of OMA formation and the effect of minerals." Mar Pollut Bull **60**(9): 1433-1441.

Zhao, L., M. C. Boufadel, X. Geng, K. Lee, T. King, B. Robinson and F. Fitzpatrick (2016). "A-DROP: A predictive model for the formation of oil particle aggregates (OPAs)." Marine pollution bulletin **106**(1-2): 245-259.

Zhao, L., M. C. Boufadel, J. Katz, G. Haspel, K. Lee, T. King and B. Robinson (2017a). "A new mechanism of sediment attachment to oil in turbulent flows: Projectile particles." Environmental science & technology **51**(19): 11020-11028.

Zhao, L., M. C. Boufadel, J. Katz, G. Haspel, K. Lee, T. King and B. Robinson (2017b). "A New Mechanism of Sediment Attachment to Oil in Turbulent Flows: Projectile Particles." Environ Sci Technol **51**(19): 11020-11028.

Zhao, L., F. Gao, M. C. Boufadel, T. King, B. Robinson, K. Lee and R. Conmy (2017c). "Oil jet with dispersant: Macro-scale hydrodynamics and tip streaming." AIChE Journal **63**(11): 5222-5234.

Zhao, L., J. Torlapati, T. King, B. Robinson, M. C. Boufadel and K. Lee (2014). A numerical model to simulate the droplet formation process resulting from the release of diluted bitumen products in marine environment. International Oil Spill Conference Proceedings, American Petroleum Institute.

Zhao, L., B. Wang, P. M. Armenante, R. Conmy and M. C. Boufadel (2015). "Characterization of Turbulent Properties in the EPA Baffled Flask for Dispersion Effectiveness Testing." Journal of Environmental Engineering: 04015044.